Meteor stream activity

V. The Quadrantids, a very young stream

P. Jenniskens[1,2]**, H. Betlem**[2]**, M. de Lignie**[2]**, M. Langbroek**[2]**, and M. van Vliet**[2]

[1] NASA/Ames Research Center, Mail Stop 239-4, Moffett Field, CA 94035-1000, USA
[2] Dutch Meteor Society, Lederkarper 4, 2318 NB Leiden, The Netherlands

Abstract. This paper presents the first large set of precisely reduced orbits of Quadrantid meteoroids. These orbits were obtained from photographic observations during the 1995 return of the Quadrantid stream. The orbits refer to the main peak of the activity curve, with an unidentified few being part of a broad background component. The measured dispersion of orbits is less than from previous data obtained by less accurate techniques. In combination with existing stream models, we conclude that the main component is only about 500 years young, much less than the 5000-7500 year age that was widely assumed before. This main peak is now interpreted as an "outburst", with an evolution history similar to other near-comet type outbursts, while the background is thought to be the classical "annual" dust component. The stream does not originate from comet 96P/Machholz 1. Rather, the parent object may be hiding as an asteroid-like object in a high-inclination orbit. An estimate of that orbit is given.

Key words: comets – meteors, meteoroids

1. Introduction

The *Quadrantid*, or *Bootid*, shower is the most intense of all annual meteor streams when viewed under good circumstances. It was among the first to be discovered, in January 1835 (Fisher 1930, Lovell 1954), and has been the topic of many studies ever since. The shower has an exceptionally short duration (Shelton 1965). No other annual stream is known to be crossed in less than a day. The steep slope of the activity curve profile (B = $\Delta \log ZHR/\Delta\lambda_\odot \sim 2.5$ – Jenniskens 1994) is only matched by some long duration meteor outbursts (Jenniskens 1995). The stream is also one of two streams that are thought to have mass sorting along the node (Kashcheyev & Lebedinets 1960, Hughes & Taylor 1977, Bel'kovich et al. 1984), an asymetric main peak

of the activity curve (Prentice 1940, McIntosh & Simek 1984, Jenniskens 1994), and a changing mass distribution index with particle mass (Simek 1987), the other stream being the Geminids.

Observations of the Quadrantids are not abundant, because an extremely short duration of the shower conspires with bad weather conditions in early January in the northern hemisphere where the shower is exclusively observed. Moreover, the high Declination of the radiant, in combination with an unfavorable Right Ascension, causes large variations in observability for all types of observations, which are difficult to correct for.

The Quadrantid stream is the only major stream without an obvious parent body. The prevailing view is that the meteoroids were ejected from comet 96P/Machholz 1 (1986 VIII), or perhaps comet C/1491 Y1 (1491 I), thousands of years ago and came together to form a narrow stream only recently (Steel 1994). The association with comet P/Maccholz is based on the backward integration of Quadrantid-like orbits, which shows a dramatically different orbit some 1000-4000 years ago (Hamid & Youssef 1952, Babadzhanov & Zausaev 1975). Comet P/Maccholz had a similar orbit at the time (Zausaev & Pushkarev 1989, McIntosh 1990). Williams et al. (1979) proposed that the stream formed when the parent broke up 1300-1700 years ago. Babadzhanov & Obrubov (1992) went further back in time and produced 7 meteoroid streams by ejection of test particles from comet 96P/Machholz 1 some 7500 years ago, only one of which resembles the Quadrantid stream. The other proposed association, with comet C/1491 Y1 (Hasegawa 1979), is based on the presumption that this comet had a short orbital period in the 15th century. Williams & Wu (1993) found that the comet may have been perturbed into an orbit that put it outside the Quadrantid stream at about 1650 and proceeded to calculate a stream model for ejection some 5000 years ago. All present models imply that the meteoroid orbits diverged since the moment of ejection, but came together again in the last 150-200 years. The narrow width of the shower is attributed to the high orbital inclination (Shelton 1965). However, it is unclear to us how that would make the Quadrantid stream is much narrower

than, for example, the annual Lyrid stream, which has a similar high inclination orbit (Jenniskens 1994).

Our newly measured orbits of Quadrantids lead to a strikingly different picture of the stream. Preliminary orbital data were published by Betlem (1996) and de Lignie & Jobse (1996). Analysis of the results now lead us to discover that the stream is highly structured, with little dispersion for given mass and speed, implying a young age. Thus, we question the assignment of comet P/Maccholz as the parent of this meteor stream and the high age of the stream proposed in present models.

2. The observations

Clear and transparent weather conditions prevailed on January 3, 1995, which made it possible to utilize photographic, image intensified TV camera and visual meteor observing techniques at five locations in the Netherlands (Betlem et al. 1995). The meteor stations were operated by members of the Dutch Meteor Society and were located in Benningbroek (J. Nijland), Biddinghuizen (C.R. ter Kuile e.a.), Bosschenhoofd (J. van 't Leven), Oostkapelle (K. Jobse) and Rha (H. Betlem e.a.). There was no moonlight that night. Snow covered the ground and temperatures dropped to -8 degree Celsius.

2.1. Photographic data

Five photographic stations equipped with platforms of 35mm cameras with f1.8/50mm optics provided multi station images of Quadrantids of magnitude +0 and brighter. The observing technique has been described in Betlem et al. (1997).

The data were reduced by first digitizing the negatives on Kodak Photo-CD at a resolution of 3072×2048 pixels, which were then analysed with the interactive PC program Astro Record 2.0 (de Lignie 1994; 1995). The positional accuracy of the astrometrical calculations achieved with this procedure is similar to that using the JENA Astrorecord X-Y measuring machine as in Betlem et al. (1997), because the accuracy is limited by the optical quality of the cameras and the imaging of the rotating shutter breaks of the meteor trail. Atmospheric trajectory and heliocentric orbit of the meteors (Table 1), including their formal error, were calculated as in Betlem et al. (1997). This does not include possible small errors in some of the orbits caused by a wrong identification with one of the visually recorded times of bright meteors. In most cases, however, such erroneous identifications are detected by producing obvious wrong results in the plane fitting procedure.

2.2. Image intensified video camera data

Image intensified video cameras were operated from the two stations Oostkapelle (K. Jobse) and Bosschenhoofd (J. van 't Leven), which provided video footage of Quadrantids of magnitude +6 and brighter.

The camera at Oostkapelle consists of a micro-channel-plate (MCP) image intensifier with a 48 mm photo cathode (XX 1332), an f/2.0 f = 135mm objective and a Video 8 camcorder.

Table 1. Photographic orbits of Quadrantid meteors - DMS data (J2000). Tolerances refer to the least significant digit. Columns give the solar longitude ($\lambda_\odot$) = ascending node, perihelion distance (q), semimajor axis (a), inclination (i), argument of perihelion (ω), and absolute visual magnitude, i.e. at a distance of 100 km (Mv).

DMS-	$\lambda_\odot$	q	1/a	i	ω	M_v
95001	283.1239	0.974±0	0.31±3	70.8±4	167.8±3	−1
95004	283.1385	0.983 0	0.30 3	72.6 5	176.5 5	−2
95005	283.1606	0.976 0	0.36 1	71.1 2	168.5 3	−1
95006	283.1694	0.979 0	0.30 4	72.2 5	172.0 3	−2
95007	283.1780	0.979 0	0.34 3	74.0 5	171.2 4	−2
95010	283.2303	0.977 0	0.31 5	71.0 8	169.5 5	−3
95013	283.2369	0.978 0	0.33 1	71.9 2	170.4 3	−1
95014	283.2849	0.977 0	0.31 1	70.8 2	170.0 3	−4
95016	283.2970	0.980 0	0.32 1	71.2 2	172.7 1	−3
95018	283.3049	0.977 0	0.29 3	72.4 5	170.1 4	−1
95019	283.3081	0.979 0	0.30 4	72.9 6	171.6 3	−2
95020	283.3169	0.976 4	0.33 5	70.7 9	168.7 3	−3
95022	283.3396	0.979 1	0.34 7	71.0 11	171.6 7	−2
95023	283.3473	0.980 1	0.32 7	73.3 11	172.6 7	−2
95027	283.3619	0.979 1	0.28 9	72.1 14	172.1 7	−1
95028	283.3640	0.976 1	0.17 10	71.6 15	169.6 8	−0
95029	283.3663	0.980 1	0.27 12	73.3 19	173.1 8	−2
95032	283.3729	0.980 0	0.32 3	72.6 4	172.6 2	−2
95034	283.3780	0.973 1	0.25 1	71.4 13	167.8 3	−4
95036	283.3842	0.979 0	0.33 1	72.4 1	171.5 1	−2
95039	283.3950	0.981 0	0.34 2	71.1 3	173.5 5	−0
95040	283.4070	0.982 0	0.37 1	72.6 2	174.4 5	−2
95041	283.4086	0.975 1	0.33 1	71.6 2	168.3 5	−4
95043	283.4157	0.980 0	0.30 1	71.0 2	173.2 1	−2
95045	283.4186	0.976 0	0.27 4	71.8 6	169.0 6	−1
95047	283.4191	0.982 0	0.31 4	75.0 6	175.9 2	−1
95048	283.4192	0.979 0	0.39 1	73.6 2	175.6 1	−0
95050	283.4247	0.979 1	0.23 1	73.0 2	171.7 4	−2
95051	283.4259	0.975 0	0.26 5	71.9 9	168.7 7	−3
95052	283.4259	0.981 0	0.32 1	73.3 2	173.2 5	−3
95054	283.4330	0.980 0	0.30 2	72.8 3	172.3 5	−4
95058	283.4461	0.978 0	0.30 1	71.1 1	170.8 2	−2
95059	283.4468	0.979 1	0.32 5	71.1 8	171.6 6	−2
95061	283.4560	0.978 0	0.25 10	70.2 15	170.5 7	−1
95062	283.4614	0.980 0	0.33 2	72.4 3	173.0 5	−4

The camera in Bosschenhoofd is very similar in design and consists of an MCP image intensifier with a 25 mm photo cathode (XX 1400), an f/1.2 f=85 mm objective and a Hi 8 camcorder. Both cameras have a field of view of about 20 degree diameter and star limiting magnitude of +8.5. The distance between the two stations is about 70 km. The cameras were aimed at a position in the atmosphere 100 km above the Earth's surface and 106 km from the stations.

The video tapes have been visually inspected and meteors that are too faint or at the edge of the field were discarded. The images have been digitized at a resolution of 384x288 pixels, which does not further limit the image resolution. The position of the meteor trail and about 25 surrounding stars were mea-

Table 2. As Table 1. Video orbits of Quadrantid meteors - DMS data (J2000).

DMS-	$\lambda_\odot$	q	1/a	i	ω	M_v
950001	283.0141	0.979±1	0.30±3	73.4±5	171.6±7	+3
950002*	283.1543	0.964 2	0.36 3	69.8 5	161.9 9	+2
950004	283.1841	0.977 1	0.36 3	72.1 5	169.8 7	+4
950008	283.2068	0.978 1	0.31 3	71.2 5	170.7 6	+3
950009*	283.2096	0.970 3	0.45 11	69.6 21	164.3 24	+6
950012	283.2330	0.981 1	0.35 3	73.1 5	173.6 6	+4
950014*	283.2372	0.970 3	0.23 9	71.7 14	165.7 19	+3
950015	283.2372	0.981 1	0.30 5	71.9 8	173.7 8	+3
950016	283.2421	0.978 1	0.38 3	71.6 5	170.2 7	+3
950017	283.2428	0.983 0	0.30 4	73.2 6	176.8 6	+1
950018	283.2450	0.981 1	0.27 8	72.0 13	173.5 13	+4
950019	283.2493	0.977 1	0.41 3	71.5 5	169.6 8	+3
950023	283.2726	0.978 1	0.37 3	71.2 5	170.1 7	+2
950026	283.2839	0.977 1	0.32 7	71.5 11	169.5 9	+5
950027	283.2854	0.975 1	0.35 3	69.4 5	167.8 6	+3
950033	283.3037	0.974 1	0.38 3	69.5 5	166.9 6	+4
950037*	283.3321	0.961 2	0.31 10	68.9 17	160.8 16	+3
950041	283.3455	0.980 1	0.29 3	73.3 5	172.4 6	−1
950043	283.3533	0.978 1	0.38 3	70.4 5	170.1 6	+2
950045	283.3618	0.978 1	0.32 10	73.1 16	170.8 13	+3
950047	283.3709	0.979 1	0.37 3	71.2 5	171.4 6	+3
950051	283.4008	0.978 1	0.41 4	68.6 8	169.9 7	+3
950052	283.4022	0.980 1	0.29 4	74.1 7	172.3 12	+6
950053*	283.4057	0.974 1	0.35 3	71.9 5	167.5 6	+5
950056	283.4107	0.978 1	0.28 3	74.0 5	171.1 6	+2
950058	283.4135	0.979 1	0.24 6	73.0 10	171.9 6	+5
950061	283.4263	0.978 1	0.40 5	70.3 9	170.5 7	+4
950065	283.4340	0.978 1	0.49 3	68.0 6	170.0 7	+4
950067	283.4412	0.978 1	0.30 5	68.7 8	170.6 7	+5

* Outlayers in diagrams of orbital elements versus Declination.

Table 3. Photographic Quadrantid orbits from the IAU database (Eq. J2000). First two digits of code indicate the year of the Quadrantid return. An asterisk marks meteors photographed outside the main peak of activity. Data are from: (1) Whipple (1954), (2) Jacchia & Whipple (1961), (3) Hawkins & Southworth (1961), (4) Babadzhanov & Kramer (1965), (5) Lindblad (1987).

IAU-	Source	$\lambda_\odot$	q	1/a	i	ω	M_v
51-2660	(1)	282.8467	0.974	0.29	73.8	167.9	−1
54-19945	(2)	283.1507	0.970	0.33	68.6	165.2	+0
54-9953	(2)	283.1864	0.978	0.34	72.7	170.3	+0
54-9955	(2)	283.1868	0.983	0.32	72.6	180.4	+1
54-9966	(2)	283.2051	0.981	0.37	71.0	174.1	−0
54-9974	(2)	283.2193	0.978	0.33	72.5	170.4	−1
54-9983	(2)	283.2263	0.977	0.33	72.4	169.6	−1
54-9985	(2)	283.2345	0.975	0.33	70.8	168.3	−0
54-9997	(2)	283.2512	0.980	0.31	73.4	172.8	+1
54-10006*	(2)	284.2078	0.975	0.32	72.5	168.6	+0
54-1*	(3)	282.0800	0.983	0.35	72.1	177.2	+0
54-2	(3)	283.0886	0.979	0.33	70.0	171.5	+1
54-3	(3)	283.0902	0.977	0.35	71.7	170.1	+1
54-4	(3)	283.2371	0.977	0.34	73.1	169.6	+1
65-00165	(4)	283.1383	0.979	0.67	65.2	169.0	−4
65-00185	(4)	283.1763	0.976	0.65	65.4	166.2	−6
80-1*	(5)	283.7841	0.976	0.32	71.4	168.7	−6
79-1*	(5)	287.5566	0.978	0.30	71.2	170.9	−14

3. Results

Thirty-five pairs of photographic meteor images allow the calculation of planes through meteor trail and the observing site with convergence angles in excess of Q > 20 degrees, thus providing accurate orbital elements (Table 1).

Sixty-nine meteors were recorded simultaneously by the video cameras, of which 49 could be fully reduced. The radiants scatter over a large part of the visible sky, but 32 of these cluster within 20 degree from RA = 230, DEC = +50 and 29 are taken to be Quadrantids (Table 2). One of the three meteors assigned to be sporadic has a similar radiant, but a 7 km/s higher speed, a second is both 5 degrees from the mean radiant and has a 3 km/s higher speed, while the third sporadic is found 10 degrees from the mean radiant. The nearest next sporadic radiant is only at 30 degrees distance.

3.1. The velocity vectors

Each Quadrantid meteor provides the following parameters:

1. The time of the meteor.
2. The position of the radiant in Right Ascension (RA).
3. The position of the radiant in Declination (DEC).
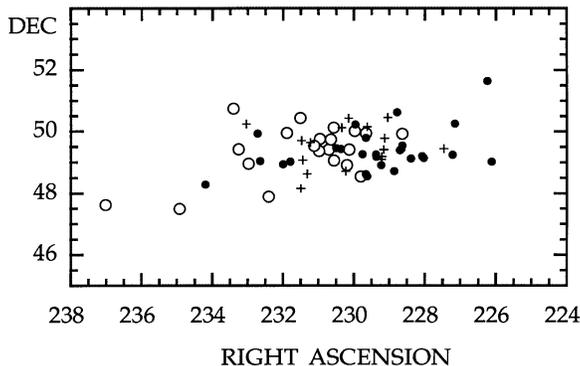4. The magnitude of the velocity vector, the speed.

sured using the same software program Astro Record 2.0. With a third-order polynomial fit, we obtained a positional accuracy of about 45″ which is a quarter of the width of a pixel of the digitized image (de Lignie 1996). Atmospheric trajectory and heliocentric orbit of the meteors (Table 2) were calculated as in Betlem et al. (1997).

The estimated random error in the orbital elements follows from the error estimates of the speed and the direction of the velocity vector (the radiant). The technique always results in favorable convergence angles for the target stream by choosing the field of view correctly. The formal error in the radiant position follows from the astrometric accuracy and the particular geometry of the trails. The estimated error in the speed is derived from the quality of the linear fit to the positions of individual images versus time, giving an average speed, and from the difference in the velocities as measured at both stations. A minimum error in the radiant of 0.3 degree and 1% in speed is applied if the algorithm specifies a lower value (de Lignie & Jobse 1996). There are no timing errors.

Fig. 1. Geocentric radiant positions after correction for zenith attraction and diurnal aberraton. Different symbols show various intervals of geocentric entry speed: o – 39.0-41.0 km/s, x – 41.0-41.5 km/s and ● – 41.5-43.0 km/s.
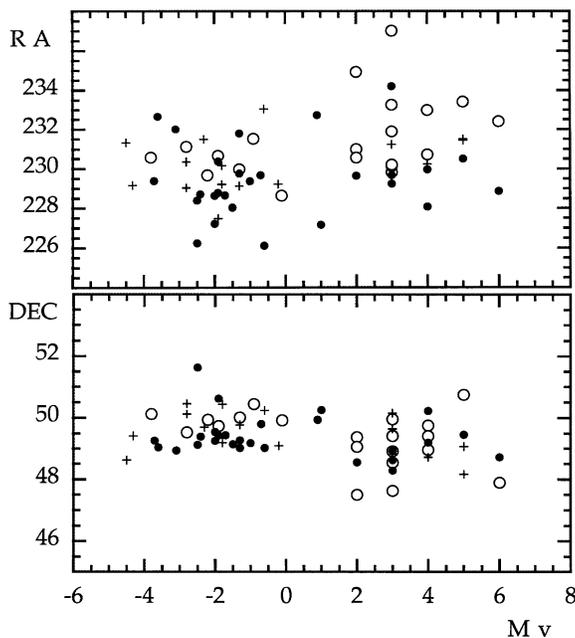

Fig. 2. The geocentric radiant position of the Quadrantids as a function of absolute visual meteor magnitude (Mv). The data are coded in three classes of speed as in Fig. 2.

The latter is expressed either with respect to the stations, corrected for atmospheric drag (V_∞), or with respect to the center of the Earth, corrected for the Earth's attraction (Vg).

Let us first consider the correlations between these parameters before examining the orbital elements calculated from them. First of all, there is a clear speed structure in the radiant distribution (Fig. 1): the higher Vg (black dots) correspond to smaller Right Ascension. That effect is present in both photographic ($M_v < 0$) and video data (Fig. 2). The photographic data show a clear sorting with Declination, the higher velocities having a lower Declination. The accuracy of the video data is not sufficient to show this same effect. The positional accuracy is $\pm 0.5^o$ for video records as compared to $\pm 0.2^o$ for typical photographic data.
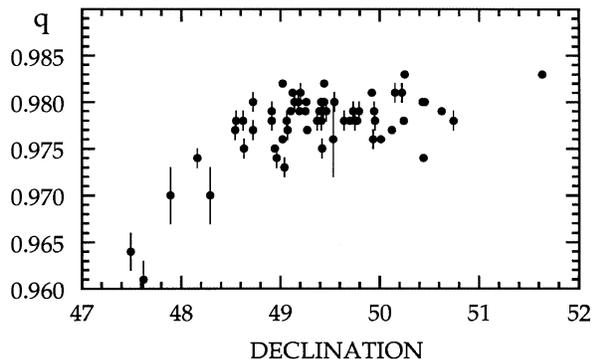

Fig. 3. Correlation of perihelion distance (q) and Declination (DEC) of the radiant for all Quadrantids. Note that orbital elements for five video orbits with DEC $< 48.2^o$ are outlayers.

Secondly, for a given range in speed, the dispersion in Declination is less than $\pm 0.3^o$, possibly fully accounted for by observational errors. That extremely small dispersion in Declination for given speed is striking. On the other hand, the dispersion in Right Ascension is large, about ± 1.2 degree (or ± 0.8 degree in RA cos(DEC)) and the same for both data sets. Hence, that dispersion is an intrinsic feature of the stream. The dispersion in RA is responsible for the large dispersion in the radiant of photographic orbits reported by Shelton (1965).

Note that the small dispersion in Declination is not a consequence of the relatively narrow range of Ω covered, because there are no strong correlations of orbital elements with Ω.

3.2. Correlations among orbital elements

The orbit of each meteoroid is described by six orbital elements: 1) perihelion distance q, 2) semimajor axis a, 3) eccentricity e, 4) inclination i, 5) argument of perihelion ω, and 6) the ascending node Ω. They are calculated from only four observed parameters. Indeed, two equations describe relationships among the orbital elements (Kresák 1976):

$$q = a[1 - e] \tag{1}$$

$$r = q[1 + e]/[1 + ecos(\omega)] \tag{2}$$

with r the heliocentric distance of the Earth at the time of the Quadrantid shower. The latter equation results from the constraint that all Quadrantids have to intersect the Earth's orbit.

The orbital parameters relate to the observed parameters as follows. The ascending node of the computed orbit is only determined by the time of the meteor. 1/a is directly dependent on Vg (at a given date):

$$Vg^2 \sim V_H^2 = GM_\odot[1/r - 1/a] \sim 1/a \tag{3}$$

The other parameters are determined by RA, DEC, and Vg. After examining correlation diagrams of the raw data with the calculated orbital elements, it is clear that a and e are only determined by the measured speed Vg, while q and ω vary only with the Right Ascension. The inclination is mainly a function

Table 4. The intrinsic dispersion (1 σ) in orbital elements of the Quadrantids (Boo) as compared to two other meteor streams, the Perseids (Per), and Geminids (Gem).

		σ Per	σ Gem	σ Boo	σ/year[*] Boo
q	AU	0.009	0.010	0.002	0.000005
1/a	AU^{-1}	0.04	0.05	0.03	0.00006
i	^{o})	1.5	2.4	1.0	0.002
ω	^{o})	2.3	1.6	2.1	0.004
$\Omega \times \sin(\epsilon')$	^{o})	1.2	0.6	0.16	0.0003

[*] yearly change assuming an age of 500 years.

of Vg, but varies also with RA and DEC. Hence:

1/a: Vg
e: Vg
i: Vg (RA, DEC)
q: RA
ω: RA
Ω: time of meteor

Part of this unique dependence on Vg, RA, and DEC is because ω is close to 180°, and hence q $\sim$ r (Eq. 2) and in a small range. Therefore, the semimajor axis a and eccentricity e strongly correlate (Eq. 1). It is less clear why ω and q are so sensitive to RA. Turning the argument around, the large dispersion in RA must reflect an intrinsic range in ω.

The independent parameters are q, a, i, and Ω. Indeed, q, a, and i do no correlate with the ascending node, there is no correlation between q and a, and only a weak trend (no strong correlation) between a and i.

This excludes five video radiants with DEC lower than 48.4 degree (marked by an asterisk in Table 2), which are found to be outlayers in the diagrams that correlate the orbital parameters with Declination (Fig. 3). No such outlayers are found in the photographic data.

3.3. Distribution of orbits in the stream

The dispersion in orbital elements, after correction for the random measurement error, can be compared directly to similar data for the Perseid and Geminid streams given by Betlem et al. (1997). The dispersion in node, perihelion distance and inclination of the Quadrantid stream (with q = 0.978 AU and ω = 179°) is significantly less than for the Perseid stream (with q = 0.953 AU and ω = 151°), but the dispersion in ω is similar. The dispersion in Ω listed in Table 4 is derived from the effective duration of the shower (Jenniskens 1994), corrected for ϵ', which is the angle between the true radiant and the apex. Note that the observed dispersion is smaller, about 0.10^o, because only half of the peak was observed.

One of our most striking results is the small dispersion of the semimajor axis (a) as compared to previous (less accurate) data sets. In fact, most orbits are confined between the 2:1 and 2:3 resonances with Jupiter at a = 2.62 and a = 3.49 AU respectively

(Fig. 4). Of the most accurate photographic orbits with $\Delta a <$ 0.1 AU, 8 out of 13 are between a = 3.0 and 3.4 AU. The five other meteors scatter over a wider range in spite of small formal errors, which should represent intrinsic dispersion (Table 4). Hence, contrary to adopted views (e.g. McBride & Hughes 1989), we find that most particles are confined in a relatively narrow range of a and are not widely dispersed inside and outside Jupiter's orbit. This is true also for the relatively small particles measured by video, down to magnitude +6 (mass 4×10^{-4} g), with particle sizes comparable to those measured by radar and discussed in previous literature.

There is a hint that orbits cluster near the 3:5, 2:3 and 1:2 resonances, most clearly seen in the accurate photographic data (Fig. 4). Unfortunately, the data do not allow a complete resolving of the resonant structure. The 8 accurate Super Schmidt orbits (Table 3) cluster near the 3:5 resonance, with 1/a = 0.33±0.01.

There is some incline for i in the photographic data to cluster in two domains at about 71.2 and 72.8 degree (Fig. 5). The same clustering is seen in a subset of data with $\Delta i < 0.3^o$ (15 meteors). The cluster with i = 71.2 is the more confined one. Because there is no instrumental reason for this, we believe this to be a true stream structure. Surprisingly, there is no correlation of these clusters with those observed in the distribution of 1/a. However, when averaging the best of orbits ($\Delta 1/a < 0.03$ AU^{-1}), there is a trend of decreasing i with decreasing a: the mean inclination is i = 72.8 at the 2:3 resonance, 71.9 at the 3:5 resonance and 71.4 at the 2:1 resonance.

Finally, there is the oddity of a weak trend between ω and Ω, which is not apparent in the perihelion distance q.

3.4. Dependence on meteor mass

Let us now consider the variation of orbital elements with a fifth free parameter: the magnitude of the meteors (or mass of the meteoroids).

Brightness estimates for photographed meteors are those of the visual observers, and are corrected to a common distance of 100 km. A similar absolute brightness of the video meteors was derived by comparing the meteor with the surrounding reference stars while it moves across the screen (de Lignie & Jobse 1996).

From Fig. 2, we find a systematic difference between the radiant of bright and faint meteors. The faint video meteors have a slightly higher average Right Ascension and somewhat smaller mean Declination: $< RA >$ differs by +0.5 degree, $< DEC >$ by –0.4 degree.

We also find a weak correlation with semimajor axis a and inclination i (Fig. 4), but not with q, ω or the ascending node. The fact that only a and i correlate with mass suggests that the correlation is mainly a manifestation of differences in Vg, whereby the video meteors move –0.7 km/s slower than the photographic meteors on average.

A small systematic differences in Vg calls for closer examination of the speed measurements, because of an uncertain correction from the measured mean spead to the pre-atmospheric speed. That correction can not be measured from video records
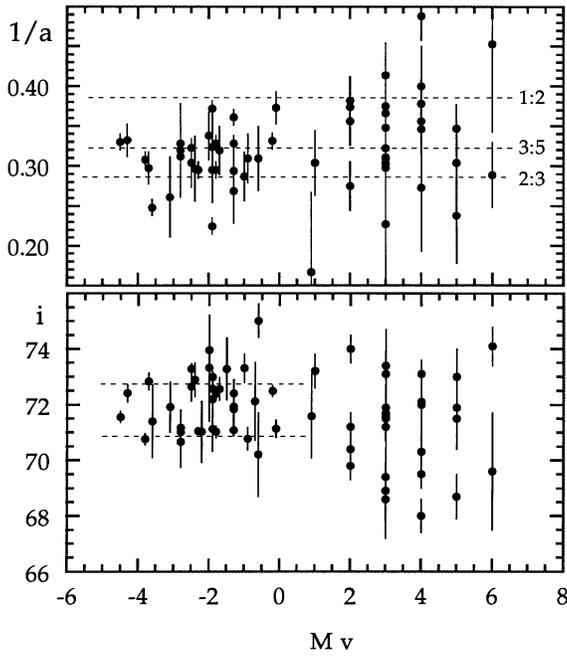
Fig. 4. Semimajor axis (a) and inclination (i) as a function of meteor magnitude. Resonances with Jupiter are marked in the upper graph, while dashed lines the lower graph guide the eye to two clusters of inclinations.
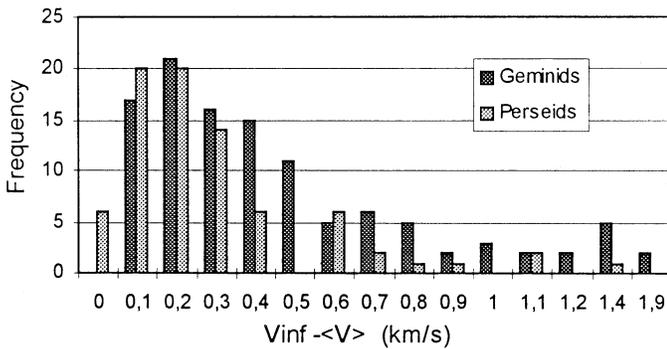

Fig. 5. Frequency distribution of the differences between the calculated values of the pre-atmospheric speed, V_{inf}, and the average speed, $< V >$, for a large number of Geminid and Perseid meteors photographed by DMS (From: de Lignie & Jobse 1995).

and is inferred from photographic records. Fig. 5 shows these atmospheric drag corrections measured for a large sample of photographed Perseid and Geminid meteors (de Lignie & Jobse 1995). The correction for video data is certainly less than that, because the video meteors are typically observed at higher altitude. It is clear that a difference in speed of as much as –0.7 km/s between video and photographic meteors is significant, more so because a relatively high constant correction of +0.3 km/s was adopted for the video records.

Table 5. Rate of change of mean orbital elements from the comparisson of IAU (1954) and DMS (1995) data.

		$\Delta/\Delta t$ yr^{-1}	$\Delta/\Delta t$ [1] yr^{-1}
q	AU	< 0.00005	$+0.0012$
1/a	AU^{-1}	$+0.0005\ (\pm2)$	$+0.00018$
i	^{o}	< 0.014	$+0.004$
ω	^{o}	< 0.038	$+0.017$
Ω	^{o}	$-0.0009\ (\pm2)$	-0.0049

[1]: Rate of change of orbital elements as calculated by Hughes et al. (1981).

3.5. Change of orbital elements over time

The mean orbit of photographed and filmed Quadrantids compares well with the 18 precisely reduced photographic orbits in the IAU Database, (Lindblad 1987, Wu & Williams 1992), except for two outlayers from a paper by Babadzhanov & Kramer (1965). The IAU Database orbits are reproduced in Table 3. Most results were obtained in the year 1954 (Shelton 1965). There is no significant difference. Hence, our results do not confirm the large change in orbital elements over time reported by Ohtsuka et al. (1993) and also deviate significantly from orbital elements published by Koseki (1989), presumably because these data have not been reduced precisely.

Comparison of IAU and DMS data leads to the yearly change of orbital elements listed in Table 5. The precession of the ascending node $\Delta\Omega/\Delta t$ is derived from the yearly shift of the time of maximum activity (Hawkins & Southworth 1958, Hughes 1972, Hughes et al. 1979, McIntosh & Simek 1984).

4. Discussion

4.1. Two dust components in the activity profile

The activity curve of the annual Quadrantid stream is well known (e.g. Bel'kovich et al. 1984, McIntosh & Simek 1984, Simek & McIntosh 1991, Rendtel et al. 1993). The activity curve consists of a narrow peak and a broad background component (Jenniskens 1994), which are drawn schematically in Fig. 6 (top). In order to illustrate for which part of the curve we obtained photographic data, we show superposed the visual observations obtained during the 1995 return (Langbroek 1995, van Vliet 1995). We find that our observations cover about half of the narrow main peak of the activity curve, slightly favoring the ascending branch. Most observations were obtained at the peak of the shower, between solar longitude 283.2 and 283.4 in the second half of the night when the radiant was most favorable.

A similar two-component picture emerges from the reported size distribution of particles in the shower. Various publications have reported mass sorting in the narrow peak, whereby brighter meteors are thought to come later than the fainter ones (Kashcheyev & Lebedinets 1960, Hindley 1970; 1971, Hughes 1972). However, that conclusion is not supported by recent stud-
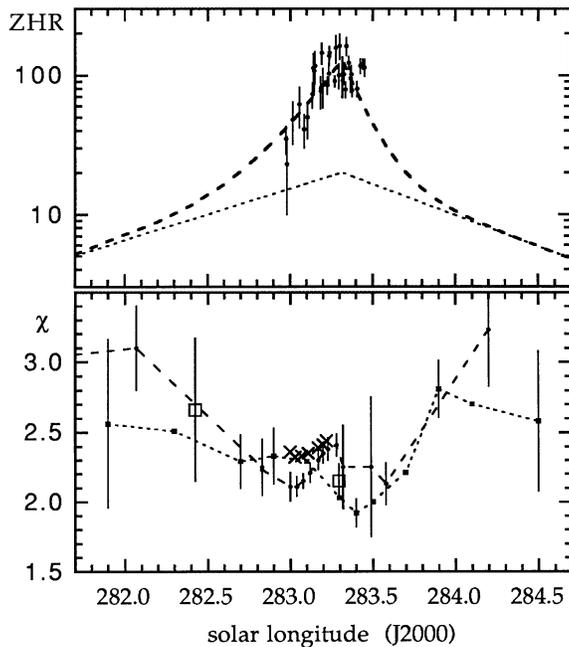
Fig. 6. Top: Zenith Hourly Rate of the 1995 Quadrantids from visual observations during the night of January 3. Dashed lines show the main and background component in the meteor activity curve derived by Jenniskens (1994). Bottom: The magnitude distribution index (χ) across the stream activity profile, in a compilation from results by • – Bel'kovich et al. (1984), square – Veltman (1987) and o – Rendtel et al. (1993). Values by Rendtel et al. have been corrected for the dependence of χ on zenith angle distance by Bellot Rubio ($\times$ – 1994).

ies. Notably, McIntosh & Simek (1984) and Simek & McIntosh (1991) did not find a strong difference in the width or time of maximum between faint and bright meteors. They also found that the mass sorting was sometimes in the opposite direction. Bellot Rubio (1994) showed that part of the reported variation in the magnitude distribution index:

$$\chi = n(m + 1)/n(m) \tag{4}$$

is due to the radiant zenith angle dependence of the mean magnitude. We have gathered estimates of χ found in the literature in Fig. 6 (Rendtel et al. 1992, Bel'kovich et al. 1984, Veltman 1987). Poole et al. (1972) found $\chi = 1.8 \pm 0.1$ for the main peak meteors. Crosses in Fig. 6 show the corrected values of Rendtel et al. as given by Bellot Rubio (1994), which illustrate the effect of a changing radiant altitude. The data are consistent with the magnitude distribution index χ following the decomposition of the activity curve in two components as found in Jenniskens (1994). Hence, the narrow main peak is relatively rich in bright meteors compared to the broad background component.

4.2. The "outburst" Quadrantids: the main peak

4.2.1. The epoch of ejection

The small dispersion of orbital elements argues against models in which the meteoroids were ejected thousands of years ago

by comet 96P/Machholz 1 or comet C/1491 Y1 and came together only in recent years (Williams et al. 1979, Babadzhanov & Obrubov 1992, Wu & Williams 1992). Comparison with model calculations show that as little as 500 years of perturbations are sufficient to cause a larger dispersion than observed in the inclination, the perihelion distance and the aphelion distance of Quadrantid orbits (Williams et al. 1979, Froeschle & Scholl 1986). Hence, the epoch of ejection must have been less than about 500 years ago.

Similarly, the relatively small amount of mass sorting (if any) in the stream argues against an old age, with a low inclination at earlier times. In that case, mass sorting would have been rapid because there should have been an intrinsic variation of aphelion distances with meteor mass during stream formation (Hughes et al. 1981). We would have expected strong correlations of the orbital elements with 1/a, which are not observed.

On the other hand, the epoch of ejection can also not have been much more recent than 500 years, because the Quadrantids are spread almost homogeneously along their orbit (McIntosh & Simek 1984). From Whipple's (1951) ejection model, Hughes (1986) estimated a loop closure time for meteors of magnitude +2 of about 1050 years. If the ejection velocities calculated from Whipple's formula are correct and the stream is younger than 500 years, then some nonhomogeneity must still exist in the Quadrantid stream, especially for the bright meteors. A periodic variation in particle size distribution of the main peak should result. Moreover, the mean particle size distribution from observations gathered over a number of years would not be exponential over its whole mass range in that case, because the bright meteors would not be sampled as well as the faint meteors.

Indeed, Simek (1987) reported a gradual decrease of χ with increasing meteor magnitude for radar echoes of Quadrantid meteors collected over a number of years. That change of χ with magnitude is consistent with the ejecta of the Quadrantids being relatively young compared to the loop closure time. Dark dots in Fig. 7 show the ratio of Quadrantid over sporadic meteors for given magnitude class from Simek (1987). The counts suggest a lack of negative magnitude Quadrantids compared to the distribution expected for a constant χ. Our photographic data for the single return of 1995 do not confirm the magnitude of this effect. However, photographic, visual and video data together do suggest a gradual decrease of χ with increasing magnitude: from least-squares fitting, we find $\chi = 3.1$, $\chi = 2.7$, and $\chi = 1.7$ respectively, assuming that the sporadic $\chi_s = 3.4$ (Kresáková 1966). The mean slope of $\chi = 2.2$ (dashed line in Fig. 7) is consistent with values of χ reported in the literature (Fig. 6) and implies that the main peak is relatively poor in faint meteors as compared to other annual streams, for which χ is typically 2.5-3.1 (Kresáková 1966, Jenniskens 1994).

4.2.2. The signature of the ejection process

Young ejecta are thought to be responsible for meteor outbursts, which are transient enhancements of meteor rates on top of the normal annual rates (Jenniskens 1995). Although the Quadran-
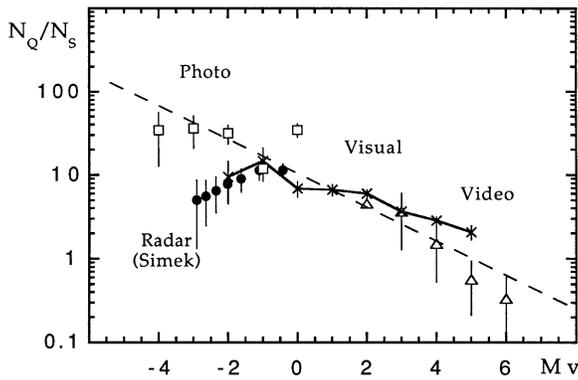
Fig. 7. The number of Quadrantids over the number of sporadic meteors observed in various intervals of visual magnitude. The slope in the diagram is proportional to χ (Fig. 5). Photographic, visual and video data for the 1995 Quadrantid return are compared to radar data by Simek (1987).

tids can be detected in all years, the main peak of the stream does have some features of meteor outbursts.

First of all, the Quadrantid particles show some characteristics of relatively fresh cometary material. Jacchia et al. (1967) studied 10 Quadrantids from precisely reduced SuperSchmidt images. The fragmentation index has the highest value among a group of meteor streams, only the value derived from two outburst Draconids is higher.

Secondly, the current width of the stream is comparable to that of the early Leonid outbursts and those of the Phoenicids and Orionids, as well as background components of the Draconids and Andromedids, which all have B~1. The relatively low value of $\chi = 2.2$ is also reminiscent of various outbursts: the i-Draconids, Puppids, the recent Perseid outbursts (Jenniskens 1995, Brown & Rendtel 1996) and the broad early Leonid outbursts (Jenniskens 1996).

Finally, the total mass of the main peak is 0.06 ± 0.02 $\times 10^{15}$g, and compares well to the mass of dust features that cause near-comet type outbursts: i.e. 0.006, 0.006, and 0.03 $\times 10^{15}$ g for the i-Draconids, the Draconids and the Andromedids respectively, and far-comet type outbursts: 0.07 and 0.06 $\times 10^{15}$ g for the Lyrids and alpha-Aurigids (Jenniskens 1995). Given a typical mass loss rate, this suggests that the Quadrantid main peak is the result of only 10 or so perihelion passages, during an interval of activity of perhaps 60 years.

If so, then the fact that the Quadrantids do not vary in total activity much from year to year implies that the parent object has ceased to deposit new dust in this component for much of the time since initial ejection, presumably because the comet has been inactive.

4.2.3. Planetary perturbations

The large dispersion in ω and small dispersion in q, and consequently the large dispersion in Right Ascension of the radiant, are best explained by planetary perturbations by Jupiter. Shelton (1965) pointed out that Jupiter's influence at the other node

of the orbit causes the stream to have a stable node, but large variations in ω and i.

Indeed, the observed stream width is certainly broader than expected based on the ejection process itself and some additional dispersion by planetary perturbations is implicated. For example, the spread in semimajor axis would suggest ejection velocities of as much as $V_{ej} = 100\text{-}300$ m/s, assuming isotropic emission and (Hughes 1977, McBride & Hughes 1989):

$$\Delta a = 2.26 \times 10^{-3} a_c^2 V_c V_{ej} cos(\phi) \tag{5}$$

with the comet heliocentric velocity V_c of 39.1 km/s, the comet semimajor axis $a_c = 3.14$ AU and cos $(\phi) = 1$ for $\Delta a = 0.25$ AU. Such large ejection velocities are unlikely for a comet with q close to 1 AU (Whipple 1951), and are inconsistent with recent models of comet dust trail formation that suggest $V_{ej} = 1\text{-}10$ m/s (Sykes et al. 1986; 1990, Sykes & Walker 1992).

Also, there is no clear effect of radiation pressure in the distribution of semi-major axis in the data (Kresák 1976). Hughes et al. (1981) calculated the expected difference in Q for 0 and +7 meteors to be about 0.03 AU. We do not observe such difference. The measured difference between photographic and video meteors (if any) is Δ a = 0.04 AU, but not in the correct sense: the weaker meteors seem to have a smaller aphelion distance (Q ~ 4.50 AU) than the brighter ones (Q ~ 5.18 AU). Presumably, the effect is lost by additional dispersion.

The width of the main peak may perhaps reflect the oscillations of the descending node near the Earth's orbit, as mirrored by the Sun's reflex motion. For long period comets, that oscillation is of order ±0.010 AU (Jenniskens 1997). Hence, if the particles are dispersed into new orbits with a similar nodal dispersion as the scatter in nodes due to the planetary perturbations, then the stream width expected is about B~1.1. That is, if the influence is from all planets together, or B~2.2 if the influence is mainly that of Jupiter. Indeed, the latter value is close to the observed value of B ~ 2.5 (Jenniskens 1994).

4.2.4. Comparison to model calculatons

Various numerical models have been developed to study the planetary perturbations on the Quadrantid stream, most of which are thought to apply to the main peak. They typically predict a fast orbital evolution (Williams et al. 1979, Hughes et al. 1981). For example, Table 5 lists computed values by Hughes et al. (1981) for the mean rate of change of orbital elements of the Quadrantid stream between AD 1830 and 2030. The measured rate of change of the perihelium distance and the precession of the node are smaller than calculated. Other orbital elements may change more gradually too, but have a relatively large measurment uncertainty.

The models are flawed by an assumed large observed dispersion in the stream. For example, the observed rate of nodal regression is smaller than the computed value and also the change in perihelion distance is less than predicted. Apparently, particles do not typically come close to Jupiter, either because of smaller aphelion distances than assumed or because the particles are trapped in mean motion resonances with the planets

(Wu & Williams 1995). Wu & Williams found from model calculations of the Perseid stream that particles trapped in mean motion resonances tend to spend significant time on orbits close to the resonance, evolving for a short period in a more chaotic behavior and then settling again onto an orbit close to another resonance.

Another explanation for observed differences are selection effects caused by the Earth's path through the stream. The models predict a strong variation over the years in the peak activity of the Quadrantids (Murray et al. 1980). Such variation is not observed (Prentice 1940, Bel'kovich et al. 1984). It is possible that the stream is not cylindrical and the Earth crosses different parts of the stream in successive years, while the stream itself does evolve as calculated. With q increasing and Ω decreasing, his would be a similar situation as proposed for the Gemind shower (Fox et al. 1982).

Numerical models by Hughes et al. (1979) show an oscillation of the mean inclination (and semimajor axis) over time, with an amplitude of about 1 degree. This effect is perhaps responsible for the two clusters of i found in the data, which differ by 0.8 degree. Such is possible if the orbits remain a relatively long time at the extremes of the oscillations. However, one might expect a correlation between i and a in that case, which is not observed.

4.3. The "annual" Quadrantids: the background component

Thus far, we have only discussed the main peak. However, if the main peak is relatively fresh ejecta, then this implies that there should be a more dispersed component that would otherwise be called the "annual" stream.

That "annual" component may be the background component of Fig. 6. Arguments for this are the following: the dispersion is similar to that of other annual streams: B = 0.37±0.10 for the rising branch as compared to B = 0.35±0.03 for the Perseids (Jenniskens 1994). The magnitude distribution index $\chi = 2.6$-3.0 is similar to that of other annual streams, with a typical value of $\chi = 2.5$-2.7 (Jenniskens 1994). The total mass in the background component (0.4×10^{15} g) is in the same order of magnitude as that of many other annual streams (Jenniskens 1994). Finally, the background component is symmetric ($B^+ = 0.37 \pm 0.10$ and $B^- \sim 0.45$), unlike the background of other annual stream profiles.

There are no obvious differences in the orbits of meteors in this background (marked by an asterisk in Table 3) and the main peak of the Quadrantid activity profile. However, there are only four meteors photographed outside of the main peak; that is, before solar longitude 282.5 and after 283.7 (J2000). The only meteor photographed before the main peak, orbit 54-1 (Hawkins & Southworth 1961), has an anomalously high longitude of perihelion. It is not clear if that is a characteristic feature. Two very bright fireballs were photographed after the main peak. That, too, may not mean anything.

For certain, the "annual" stream is not merely composed of the same population of grains in the young "outburst". The magnitude distribution index in both components differ, while planetary perturbations, even chaotic motion (Gonczi et al. 1992), are not mass dependent. Either the grains fragment over time, increasing the population of small grains, or the "outburst" main peak of the Quadrantids represents only a subset of all ejecta from the parent comet. The latter explanation is the more likely. Note that a similar difference in particle size distribution has been noticed for other near-comet type outbursts, such as those of the Perseids and Leonids (Jenniskens 1995, 1997).

The simulations by Williams & Wu (1993) resulted in a stream with a dispersion of 3-4 degree in node as a result of thousands of years of long range perturbations by the planets. That order of dispersion is the same as displayed by the "annual" stream component in Fig. 6. The age of the "annual" stream can be inferred from the different dispersion of the background and main peak in the Quadrantid profile, assuming that the rate of dispersion by planetary perturbations is similar. If the "outburst" dust was ejected 500 years ago, then the "annual" stream dust is about 3400 years old. However, it is not certain that the assumption of a similar rate of dispersion is correct or can be extrapolated in time.

4.4. The parent body

Ejection as recent as 500 years ago excludes the possibility that comet 96P/Machholz 1 is the parent object, because that comet is in a much different orbit now. It is possible, however, that the Quadrantid parent was observed from Earth as a comet in historic times. Hasegawa (1979) proposed that comet C/1491 Y1 is the parent. This comet is not well observed and only a parabolic orbit has been calculated. Williams & Wu (1993) note that the orbit of the Quadrantids was roughly similar to the orbit of the comet in 1491, assuming it was of short period at that time. A sighting in 1385 may have been the same comet. In that case, calculations show that a strong change in the orbit could have occurred in 1650, which would have put the comet in a much different orbit outside of the current stream. Hence, it is possible that the Quadrantids originated from comet C/1491 Y1 in the period 1385-1491 (prior to 1650). However, it remains to be seen that comet C/1491 Y1 was indeed of short period. Moreover, it is hard to understand why most of the stream itself was not perturbed during the close encounter with Jupiter around 1650.

In our opinion, it is likely that the parent object has not been perturbed from its recent course and is hidden from view by posing as an asteroid. Although this is a near-Earth object, it has a high inclination orbit, which avoids the usual search areas for near-Earth objects in the sky. The most likely orbit is perhaps given by the cluster of 8 photographed meteors with $70.8 < i < 71.2$ and $\Delta i < 0.8$ degree. The mean of those orbits is (J2000):

q = 0.979±0.002 AU
a = 3.14±0.19 AU
i = 71.05±0.12 degree
ω = 171.2±1.8 degree
Ω = 283.3±0.1 degree

The parent body is expected to have similar but not identical

orbital elements. If the Geminid parent is any indication, then q and a should be close to the values given, but the difference may be up to several degrees in node and inclination.

The location of the parent might be derived if small variations in the peak activity of bright Quadrantid meteors could be established. Indeed, Rendtel et al. (1993) pointed out that rich returns in 1992, 1987, 1970 and 1965 may be fitted by a 5.37 year period (a = 3.067). In that case, the object should return in the first half of 1997 and again in 2002, and our observations of the stream were obtained when the comet was near aphelion. Although such variations in activity from year to year have been reported before, and various periodicities have been suggested (Prentice 1953, Bel'kovich et al. 1974, McIntosh & Simek 1984), the uncertainty in all these data is large and the significance of this result is difficult to assess.

The remaining object may still be fairly large, given that about half the original nucleus should remain (Hughes & McBride 1989). The total mass of matter in the Quadrantid stream is 0.47×10^{15} g (Jenniskens 1994), which implies that the parent was at least 660 m in diameter at some early point in time (assuming a density 1 g/cm^3). Hughes (1986) uses similar arguments to find a diameter of some 830 meters. Our result is in good agreement.

5. Conclusions

The Quadrantid shower consists of two components: a narrow peak and a broad background.

New orbital elements of the main peak show that there is structure in the velocity vector distribution of Quadrantid meteoroids intersecting the Earth's path. The fast meteors are systematically at lower Declination and lower Right Ascension. The dispersion in Declination is small, < 0.3 degree for a small interval in speed, but the dispersion in Right Ascension is significant at all speeds: ±1.2 degree.

The small dispersion in Declination implies a young age for the ejecta in the main peak of the Quadrantid shower. Comparison with existing models implies an age in the order of 500 years. The large dispersion in right ascension reflects an intrinsic range of ω, and is due to planetary perturbations by Jupiter at the other node of the orbit.

The semimajor axis of the photographic Quadrantids are in a narrow range between the 2:3 and 1:2 orbital period resonances with Jupiter. There is some indication that the orbits cluster near the 3:5 and 2:3 (and 1:2) orbital resonances, which would confirm that particles tend to spend a large part of their time near orbital resonances.

The inclination of the accurate photographic orbits are clustered near 71.1 and 72.8 degree. The clustering does not coincide with the clustering in the 1/a distribution near the 3:5 and 2:3 resonances. Its origin may be an oscillation of orbital elements seen in the models of Hughes et al. (1979).

Mass sorting is observed with 1/a and i. Contrary to previous opinion, there is no mass sorting with descending node in the main peak. Instead, we find that the main peak is relatively rich in bright Quadrantids compared to the background component.

There is some evidence elsewhere in the literature of a relative lack of Quadrantids of negative magnitudes, which may be caused by the stream being younger than the loop closure time for bright meteors. Our 1995 data suggest a more continuous size distribution.

We conclude that the main peak represents an "outburst" component, much like other near-comet type outbursts, while the background component is the classical "annual" stream. The width of the main peak (B = 2.5) may reflect the scatter in nodes due to planetary perturbations by Jupiter alone (B = 2.2) as mirrored in the Sun's reflex motion.

These observations are not consistent with models that assume that the "outburst" dust was ejected from a parent body more than about 500 years ago. Hence, an origin from comet 96P/Machholz 1, which is now in a much different orbit, is excluded. Rather, the parent may hide as an asteroidal object in a high inclination orbit. The observations leave open the possibility that the parent is comet C/1491 Y1, but it is not likely that the comet was perturbed out of the Quadrantid stream. Instead, we believe that the parent object is still associated with the stream and hides as an inactive asteroid-like object.

Future work should concentrate on following the predicted abundance variations of bright meteors during one mean orbit, in order to determine the time that the parent object passes perihelion and to put further constraints on the ejection epoch.

References

Babadzhanov P.B., Kramer E.N., 1965, Smits. Contr. Astrophys. 11, 67

Babadzhanov P.B., Zausaev A.F., 1975, Bull. Inst. Astrofiz. Tadzh. SSR 65, 40

Babadzhanov P.B., Obrubov Yu. V., 1992, in: Asteroids Comets Meteors 1991, A. Harris, E. Bowell (eds.), Lunar and Planetary Institute, Houston, p. 27

Bel'kovich O.I., Sulejmanov N.I., Tokhtas'ev V.S., 1984, BAC 35, 123

Bellot Rubio L.R., 1994, WGN, the Journal of IMO 22, 13

Betlem H., ter Kuile C.R., Johannink C., Jobse K., 1995, Radiant, the Journal of DMS 17, 16

Betlem H., 1996, Radiant, the Journal of DMS 18, 4

Betlem H., ter Kuile C.R., de Lignie M., van 't Leven J., Jobse K., Miskotte K., Jenniskens P., 1997, A& AS (in press)

Brown P., Rendtel J., 1996, Icarus 124, 414

Fox K., Williams I.P., Hughes D.W., 1982, MNRAS 200, 199

Froeschle Cl., Scholl H., 1986, in: Asteroids Comets Meteors II, Lagerkvist C.-I., Lindblad B.A., Lundstedt H., Rickman H., eds., Uppsala University, p. 555

Gonczi F., Rickman H., Froeschle Cl., 1992, MNRAS 254, 627
Hamid S.E., Youssef M.N., 1963, Smits. Contr. Astrophys. 7, 309
Hasegawa I., 1979, PASJ 31, 257
Hawkins G.S., Southworth R.B., 1958, Smith. Contr. Astrophys. 3,1
Hawkins G.S., Southworth R.B., 1961, Smits. Contr. Astrophys. 4, 85
Hindley K.B., 1970, JBAA 80, 476
Hindley K.B., 1971, JBAA 82, 57
Hughes D.W., 1972, The Observatory 92, 41
Hughes D.W., 1977, Space Res. 17, 565
Hughes D.W., Taylor I.W., 1977, MNRAS 181, 517
Hughes D.W., Williams I.P., Murray C.D., 1979, MNRAS 189, 493
Hughes D.W., Williams I.P., Fox K., 1981, MNRAS 195, 725
Hughes D.W., 1986, Asteroids, Comets, Meteors II, C.-I. Lagerkvist,
    B.A. Lindblad, H. Lundstedt, H. Rickman, Uppsala University, Up-
    psala, p. 503
Hughes D.W., McBride N., 1989, MNRAS 240, 73
Jacchia L.G., Whipple F.L., 1961, Smits. Cont. to Astrophys. 4, 97
Jacchia L.G., Verniani F., Briggs R.E., 1967, Smits. Cont. Astrophys.
    10,1
Jenniskens P., 1994, A&A 287, 990
Jenniskens P., 1995, A&A 295, 206
Jenniskens P., 1996, Meteoritics & Planetary Science 31, 177
Jenniskens P., 1997, A&A 317, 953
Kashcheyev B.L., Lebedinets N.V., 1960, Astron. Zh. 37, 119
Koseki M., 1989, in: Asteroids Comets Meteors III, C.-I. Lagerkvist, H.
    Rickman, B.A. Lindblad, M. Lindgren (eds.), Uppsala University,
    547
Kresák L., 1976, BAC 27, 35
Kresáková M., 1966, Contr. Astron. Obs. Skalnate Pleso 3, 75
Langbroek M., 1995, WGN, the Journal of IMO 23, 20
de Lignie M., 1994, Radiant, the Journal of DMS 16, 5
de Lignie M., 1995, Radiant, the Journal of DMS 17, 61
de Lignie M., Jobse K., 1995, Radiant, the Journal of DMS 17, 99
de Lignie M., 1996, Radiant, the Journal of DMS 18, 30
de Lignie M., Jobse K., 1996, WGN, the Journal of IMO 24, 20
Lindblad B.A., 1987, in Interplanetary Matter, Proc. 10th European
    Reg. Meeting of the IAU, Z. Ceplecha, P. Pecina (eds.), Vol. 2, 201

Lovell A.C.B., 1954, Meteor Astronomy, Oxford Clarendon Press,
    p.326
McBride N., Hughes D.W., 1989, in: Asteroids Comets Meteors III,
    C.-I. Lagerkvist, H. Rickman, B.A. Lindblad, M. Lindgren (eds.),
    Uppsala University, 555
McIntosh B.A., Simek M., 1984, BAC 35, 14
McIntosh B.A., 1990, Icarus 86, 299
Murray C.D., Hughes D.W., Williams I.P., 1980, MNRAS 190, 733
Ohtsuka K., Yoshikawa M., Watanabe J.-I., 1993, in: Meteoroids and
    their parent bodies, J. Stohl and I.P. Williams (eds.), p. 73
Poole L.M.G., Hughes D.W., Kaiser T.R., 1972, MNRAS 156, 223
Prentice J.P.M., 1940, JBAA 51, 19
Prentice J.P.M., 1953, JBAA 63, 175
Rendtel J., Koschack R., Arlt R., 1993, WGN, the Journal of IMO 21,
    97
Shelton J.W., 1965, AJ 70, 337
Simek M., 1987, BAC 38, 80
Simek M., McIntosh B.A., 1991, BAC 42, 124
Steel D., 1994, in Asteroids Comets Meteors 1993, IAU Symp. 160,
    A. Milani et al. (eds.), Kluwer Dordrecht, p. 111
Sykes M.V., Lebofsky L.A., Hunten D.M., Low F.J., 1986, Science
    232, 1115
Sykes M.V., Lien D.J., Walker R.G., 1990, ICARUS 86, 236
Sykes M.V., Walker R.G., 1992, ICARUS 95, 180
Veltman R., 1987, Radiant, the Journal of DMS 9, 18
van Vliet M., 1995, Radiant, the Journal of DMS 17, 117
Whipple F.L., 1951, ApJ 113, 464
Whipple F.L., 1954, AJ 59, 1217
Williams I.P., Murray C.D., Hughes D.W., 1979, MNRAS 289, 483
Williams I.P., Wu Z., 1993, MNRAS 264, 659
Wu Z., Williams I.P., 1992, MNRAS 259, 617
Wu Z., Williams I.P., 1995, MNRAS 276, 1017
Zausaev A.F., Pushkarev A.N., 1989, Bull. Inst. Astrofyz. 80, 18